

Stability of metallic thin films studied with a free electron model

Biao Wu¹ and Zhenyu Zhang^{2,3}

¹*Institute of Physics, Chinese Academy of Sciences, P.O. Box 603, Beijing 100080, People's Republic of China*

²*Materials Science and Technology Division, Oak Ridge National Laboratory, Oak Ridge, Tennessee 37831, USA*

³*Department of Physics and Astronomy, The University of Tennessee, Knoxville, Tennessee 37996, USA*

(Received 24 July 2007; published 10 January 2008)

The stability of metallic thin films is studied with a free electron model, which is popularly known as the model of “particle in a box.” A detailed theoretical framework is presented, along with discussion on typical metals, such as Pb, Al, Ag, Na, and Be. This simple model is found to be able to describe well the oscillation pattern of stability for continuous metallic films. In particular, it yields even-odd oscillations in the stability of Pb(111) film, consistent with both experimental observation and *ab initio* results. However, the free electron model is too crude to predict at what thickness a film is stable. Film stability is further examined with a model of “particle in a corrugated box,” where a lattice potential is added along the vertical direction of a film. The effect of lattice potential is found not substantial.

DOI: [10.1103/PhysRevB.77.035410](https://doi.org/10.1103/PhysRevB.77.035410)

PACS number(s): 68.55.-a, 73.21.Fg, 71.15.Nc

I. INTRODUCTION

There have been many experimental reports that atomically flat metallic thin films can grow on semiconductor substrates. They include Ag/GaAs(110),¹ Ag/Si(111),² Pb/Si(111)³⁻¹³ Pb/Ge(100),¹⁴ and, most recently, Pb/Ge(111).¹⁵ This interesting phenomenon is commonly attributed to quantum size effect: due to the small dimension perpendicular to a metallic film and the confinement from nonconducting interfaces, the electronic energy bands are discretized. The discretization can lead to an oscillatory dependence of the film's total energy on its thickness, instead of the linear dependence on thickness for very thick films. This oscillatory behavior implies that a thin film of certain layers may be energetically favored than other layers, opening a window of possibility that an atomically flat film form upon annealing. Recent experiments show that quantum size effect in these atomically flat films has strong influence on other properties of these films, such as superconducting T_c ,^{16,17} electron-phonon coupling,¹⁸ perpendicular upper critical field,¹⁹ adhesion,²⁰ surface diffusion,²¹ work function,²² and lattice relaxation.²³ This means that one achieves the ability to control the film properties by adjusting the film thickness.

Much of the physics involved in the quantum size effect can be well captured by the free electron model,^{24,25} also known as the model of “particle in a box.”²⁶⁻²⁸ In this model, the metallic thin film is regarded as a collection of free electrons, which are confined in the perpendicular direction by energy barriers at the two interfaces while free to move in the two lateral directions. It has been used to account for many experimental observations^{4,7,9,24} and in the study of thin film properties, such as conductivity.²⁹

In this paper, we present a detailed study of the free electron model on the stability of metallic thin films. The model is applied to metallic films, such as Pb(111), Al(111), Ag(111), Na(110), and Be(0001), which represent different classes.²⁴ On one hand, for films consisting of well-separated islands, we find that this model, in general, is incapable of explaining atomically flat metallic islands observed in

experiments.^{3,4,7} On the other hand, for continuous films, it can produce oscillations in the stability of thin films such as Pb(111) and Al(111). The oscillations imply that films of certain layer numbers are favored energetically.

In particular, the free electron model yields even-odd oscillations in the stability of Pb(111) film, which is consistent with experiments.¹⁵ These oscillations are also consistent with *ab initio* results^{10,15,30,31} in terms of both pattern and amplitude. For Al(111) films, this model predicts oscillations of a different pattern in the stability, which is yet to be verified experimentally. For Na(110), Ag(111), and Be(0001) films, the free electron model indicates that they lose their film characteristics and become bulklike quickly as their thickness grows.

In the free electron model, film interfaces with either vacuum or a semiconducting substrate are commonly modeled as steplike energy barriers. In the simplest treatment, the barrier is assumed to have an infinite height, regardless the specifics of an interface, for example, whether it is an interface with vacuum or semiconductors. In a more realistic treatment, the interface is modeled as a finite energy barrier with its height depending on the interface conditions. A finite energy barrier captures the fact that electrons can spill into the other side of the interface, which is ignored with infinite energy barrier. Our study finds that the height of an energy barrier has no substantial effect on the stability of thin films.

The stability of metallic thin films is examined further with an improved model of “particle in a corrugated box.”²⁷ In this model, a lattice potential is added along the direction perpendicular to the film (or confinement direction). We find that the lattice potential only marginally affects the film stability. Finally, we discuss briefly a possible role of Friedel oscillations of the electron density in film stability.

The paper is organized as follows. In Sec. II, we present the general theory of the free electron model in detail for the sake of self-containment of our paper, also to establish notations. In Sec. III, we discuss the criterion of film stability. The discussion is general, not limited to the free electron model. In Secs. IV and V, the stability of metallic films is discussed using different types of energy barriers with focus on five metallic films, Pb(111), Al(111), Ag(111), Na(110),

and Be(0001). In Sec. VI, the model of particle in a corrugated box is studied to examine the effect of a lattice potential on film stability. We summarize and make some general remarks in the end.

II. FREE ELECTRON MODEL

Free electron model studied here is formally known as the Sommerfeld theory, where a metal is treated as a collection of free electrons that obeys Fermi statistics.³² Although the lattice structure and the interaction between electrons are completely ignored in this model, it has been quite successful in explaining many metal properties.^{32,33}

In this paper, we apply the free electron model to metallic thin films that are either freestanding or grown on nonconducting substrates. As this is the simplest model possible, many aspects of a metallic thin film are either not accurately accounted or completely ignored. The effect of a nonconducting substrate is treated as energy barriers at interfaces; all the details, such as atom arrangements, between two different materials are ignored. Since the ionic lattice is not included in this model, all the energies involving lattice are completely ignored. These energies include the elastic energy caused by lattice mismatch at interfaces and the energy associated with surface relaxation. An immediate consequence of these omissions is that we have to be very cautious when we apply the free electron model to very thin films. For a very thin film, its interfaces or surfaces are a bigger part of the film than thicker films. This is vindicated in our later discussions, where we find that the stability of a thin film of less than 5 monolayers depends sensitively on the height of interface energy barriers. Some of the assumptions in the free electron models are backed by either experiments or *ab initio* computations. For example, in Ref. 15, lead films grown on different substrates have the same stability. In Ref. 31, the first-principles calculations show that different semiconductor substrates only “phase shift” the properties of lead films, which can be quite accurately captured with an energy barrier.

In the rest of this section, we present the detailed theory of the free electron model for metallic thin films. Many formulas involved also apply directly in the model of particle in a corrugated box. We then discuss how to treat interfaces as energy barriers.

Note that in the free electron model, the thickness of a film is allowed to change continuously, although the thickness in reality can only change monolayer by monolayer. As a result, we shall always present our results as functions of continuous film thickness as long as we do not focus on a specific metal.

A. General theory

In the free electron model, for a bulk material, the electron energy is

$$E = \frac{\hbar^2}{2m}(k_x^2 + k_y^2 + k_z^2), \quad (1)$$

where m is the free electron mass. For a thin film, due to the confinement by energy barriers at the film interfaces, the

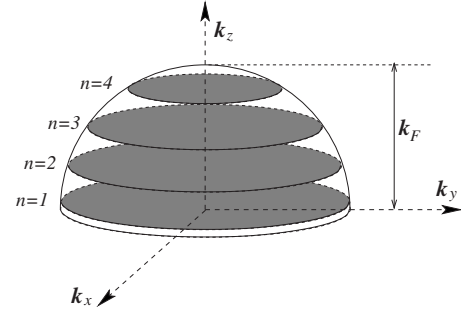


FIG. 1. Energy subbands of a metallic thin film.

energy of the film is partially discretized (see Fig. 1). If we choose the perpendicular direction as the z direction, the electron energy in a metallic film becomes

$$E = \frac{\hbar^2(k_x^2 + k_y^2)}{2m} + E_{z,n}, \quad (2)$$

where $E_{z,n}$ is the discrete eigenenergy due to the confinement along the z direction. These eigenenergies $E_{z,n}$ are determined by the energy barriers at two interfaces and the thickness of the film. Without causing confusion, we will use a simpler notation E_n for $E_{z,n}$.

For a thin film of thickness d and base area S , we have an equality for its total number of electrons,

$$\sum_{E_n \leq E_f} \frac{mS(E_f - E_n)}{\pi\hbar^2} = Sdn_0, \quad (3)$$

where E_f is the Fermi energy of the thin film and n_0 is the density of free electron in the bulk material. Let N be the highest occupied subband E_n ; we have an expression for the film Fermi energy E_f from the above equation,

$$E_f(d) = \frac{2dk_F}{3N\pi}E_F + \frac{1}{N} \sum_{n \leq N} E_n, \quad (4)$$

where E_F , k_F , and λ_F are the energy, wave number, and wavelength, respectively, at the bulk Fermi level. In arriving at the above equation, we used the identity $n_0 = k_F^3 / (3\pi^2)$ (see Ref. 32). The film Fermi energy E_f should satisfy

$$E_N \leq E_f < E_{N+1}, \quad (5)$$

which is used to determine the value of N .

Since the energy of all electrons at an occupied subband E_n is

$$\epsilon_n = \frac{m_e S}{2\pi\hbar^2}(E_f^2 - E_n^2), \quad (6)$$

the total energy of the film is

$$E_t = \sum_{n \leq N} \epsilon_n = \frac{m_e S}{2\pi\hbar^2} \sum_{n \leq N} (E_f^2 - E_n^2). \quad (7)$$

This energy E_t determines the thermodynamic stability of metallic thin films. However, for convenience of discussion (see the next section), people most of time use other forms of

energy derived from E_t . One is the energy per unit area after subtracting the bulk energy,

$$E_s(d) = (E_t - \frac{3}{5}E_F n_0 S d) / S. \quad (8)$$

Note that $3E_F/5$ is the energy per electron of bulk metals in the free electron model.³² With some algebra, we have

$$E_s(d) = \frac{k_F^2 E_F}{4\pi} \left\{ \sum_{n \leq N} \frac{E_f^2 - E_n^2}{E_F^2} - \frac{4}{5} \frac{dk_F}{\pi} \right\}. \quad (9)$$

We call E_s the film interface energy.³⁴ In the limit of thick film ($d \rightarrow \infty$), E_s is twice of the usual surface energy. Another is the energy per electron (or averaged energy),

$$E_a(L) = \frac{E_t}{S d n_0} = \frac{3\pi}{4dk_F E_{F n \leq N}} \sum (E_f^2 - E_n^2). \quad (10)$$

We will explain in the next section how E_s and E_a can be used to analyze film stability.

For simplicity, we introduce a new dimensionless parameter $\kappa = dk_F / \pi$ and rewrite the energies

$$E_f(\kappa) = E_F \left[\frac{2\kappa}{3N} + \frac{1}{N} \sum_{n \leq N} \frac{E_n}{E_F} \right], \quad (11)$$

$$E_a(\kappa) = \frac{3E_F}{4\kappa} \sum_{n \leq N} \frac{E_f^2 - E_n^2}{E_F^2}, \quad (12)$$

$$E_s(\kappa) = \frac{k_F^2 E_F}{4\pi} \left\{ \sum_{n \leq N} \frac{E_f^2 - E_n^2}{E_F^2} - \frac{4\kappa}{5} \right\}. \quad (13)$$

The dimensionless parameter κ is not only a scaled measurement of film thickness d but also is of physical meaning. It is the total phase (in units of 2π) accumulated by an electron at the Fermi level E_F traveling back and forth inside a film, which accounts for a total distance of $2d$. It is also approximately the number of nodes of the wave function for the highest occupied subband. In the limit of thick film, $d \rightarrow \infty$, one has

$$\frac{\kappa}{N} \rightarrow 1. \quad (14)$$

B. Energy barriers at interfaces

For a real metallic film, its energy barriers at interfaces are potential functions that vary quickly but smoothly over a small distance in the vicinity of interfaces. One such function can be found in Ref. 33. Nevertheless, in this paper, we will ignore this smooth change and treat energy barriers at the interfaces as step functions, as shown in Fig. 2. In this way, the metallic film is like a box containing a given number of free electrons. This is why the free electron model of metallic films is popularly known as model of particle in a box.

The energy barrier at the interface with vacuum has a height of $W_m + E_F$, where W_m is the work function of bulk metal.³³ On the substrate side, the barrier height V_0 depends on the specifics of the substrate materials.^{35,36} Since the en-

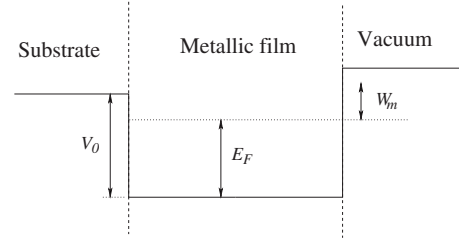


FIG. 2. Energy barriers at interfaces. The barrier at the vacuum side has a height of $E_F + W_m$; the barrier height V_0 at the substrate side depends on the specifics of the substrate material.

ergy gap is typically around 1 eV in semiconductors, it should mostly be less than 1 eV above the Fermi energy E_F of the metal. In Ref. 24, the interface between the metal and the semiconductor substrate is modeled as an infinite energy barrier with a capacitor storing the spilled charge from the metal into the substrate.

In the simplest treatment, one can assume that the energy barrier has infinite height as in Ref. 29. This treatment has many drawbacks: it ignores the specific interface conditions, treating every interface (semiconductor or vacuum) as the same; it does not allow charge spilling, which occurs at all interfaces. Despite of these inadequacies, it is still worthwhile to examine the free electron model with infinite energy barriers. The reason is that it can serve as a reference point for other more realistic treatments.

III. FILM STABILITY CRITERION

Before proceeding further with the free electron model, we pause here to discuss the criterion of film stability, that is, how to use the energies defined in the last section to determine the stability of a metallic film (or the possible outcome of annealing).

As a given amount of a certain material is deposited on a substrate, many different types of films can form. One is a continuous film seen in Fig. 3, which is the focus of this paper. During annealing at certain temperatures, the film will likely change its morphology. The driving force behind the change is thermodynamics: a system always wants to seek a morphology of lower energy when it is allowed by growth kinetics. The configuration that is a local minimum in the system energy is relatively stable and will likely be the out-

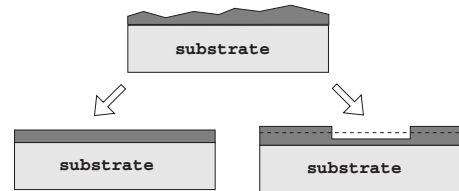


FIG. 3. Continuous thin film. The top is a rough film before annealing; after annealing, the film may become atomically flat (bottom left) or a film of two different heights (bottom right). In this case, the contact area between the film and the substrate is conserved during morphology evolution.

come of annealing. So, theoretically to find out film stability or how the film shapes up after annealing, we need to find the system energies of different configurations and compare them.

For the continuous film in Fig. 3, after annealing, the whole film may become atomically flat, having the same height everywhere, or the film may evolve to have two different heights (or other morphologies). This depends on which configuration has a lower system energy E_t . Atomically flat film is possible when $E_t(\text{left}) < E_t(\text{right})$, where $E_t(\text{left})$ and $E_t(\text{right})$ are energies for the two films at the bottom of Fig. 3, respectively. If S is the total contact area of the film with the substrate, then we have $E_t(\text{left}) = SE_s(L)$ and $E_t(\text{right}) = E_s(L+1)(S/2) + E_s(L-1)(S/2)$. Therefore, the criterion for the stability of an atomically flat film of L monolayers is

$$E_s(L) < \frac{E_s(L+1) + E_s(L-1)}{2}. \quad (15)$$

This criterion motivates us to define a new quantity, the second difference of E_s ,

$$d^2E(L) = E_s(L+1) + E_s(L-1) - 2E_s(L). \quad (16)$$

According to the criterion [Eq. (15)], a film of L monolayers is stable when $d^2E(L) > 0$ and unstable otherwise. As a film grows thicker, its properties become more and more bulklike. In other words, for a thick film, its properties should change little with an addition or removal of 1 monolayer. Therefore, we expect that for large L , the second difference d^2E is very small, $|d^2E(L)| \ll 1$. Reversely, when we have $|d^2E(L)| \ll 1$ for a given layer number, we say that the film of L monolayers is bulklike in terms of stability. The films grown in Refs. 1 and 15 are continuous films.

Caution is needed in applying the stability criterion [Eq. (15)]. It indicates mathematically that the interface energy $E_s(\kappa)$ as a function of film thickness is convex only locally for a film of L monolayers; it does not imply that the film is also stable against other configurations, such as a film of both $L+2$ and $L-2$ monolayers. For the criterion to be applicable, $E_s(\kappa)$ needs to be globally a convex function. Fortunately, the interface energy E_s is indeed a convex function globally for a metallic film (see, e.g., Fig. 6) if one would ignore the small oscillations caused by the band discretization. As we shall see later, these small oscillations can make the function $E_s(\kappa)$ concave locally, rendering films of certain thickness unstable. We note that, to our knowledge, the criterion is first used in Ref. 24 and applied again in Ref. 37.

Another interesting type of thin film consists of well-separated islands, as shown in Fig. 4. Upon annealing, one possible outcome is that all the islands evolve to have the same height. This island film has two crucial differences from the continuous film. The first difference is that the islands have different contact areas after the annealing. For a film grown on a substrate, the system energy has two parts: one is associated with the film itself, and the other comes from the change in the substrate surface caused by the growing film. For a continuous film, since the contact area is conserved during morphology evolution, the second part is



FIG. 4. Well-separated islands in a thin film. After annealing, the islands may evolve to have the same height as indicated by dashed-lined objects. As the total volume of the film is conserved, the total contact area of the islands with the substrate is changed.

always the same and can be ignored. For films of islands, the second part changes during annealing and cannot be ignored as easily as for continuous films. As the theory of the free electron model deals only with energy of the film part, it does not apply for films of islands strictly.

The second difference is the energy associated with the side faces of a film. Let us call it side energy. For a continuous film, this side energy is negligible because the side faces are very small compared to the interfaces. For a film of islands, these side faces are no longer small and have to be taken into account. To account for its effect, one has to study a model of electrons in a three-dimensional box, which is beyond the scope of this current paper that deals with only electrons confined in a one-dimensional box.

Despite the two distinctions, we nevertheless apply our model to the film of islands for the sake of knowing how well (or bad) this model is for this case. For this case, as the volume of the islands is conserved, an alternative form of energy, the energy per electron E_a , can be used as a criterion: an island of L monolayers is preferred if

$$E_a(L) < E_a(L \pm 1). \quad (17)$$

Experiments in Refs. 3, 4, and 7 reported the formation of Pb islands of preferred heights; the films in these experiments belong to this case.

IV. INFINITE ENERGY BARRIER

As a start, we treat the interfaces as infinite energy barriers. In this case, the subband energy is

$$E_n = \frac{n^2 \pi^2 \hbar^2}{2md^2} = \frac{n^2}{\kappa^2} E_F. \quad (18)$$

Plugging these energies into the formula derived in Sec. II, we have the film Fermi energy

$$E_f(\kappa) = E_F \left[\frac{2\kappa}{3N} + \frac{(N+1)(2N+1)}{6\kappa^2} \right], \quad (19)$$

the energy per electron

$$E_a(\kappa) = \frac{3E_F}{4} \mathcal{S}, \quad (20)$$

and the film interface energy

$$E_s(\kappa) = \frac{k_F^2 E_F}{4\pi} \kappa \left\{ \mathcal{S} - \frac{4}{5} \right\}. \quad (21)$$

The dimensionless variable \mathcal{S} is given by

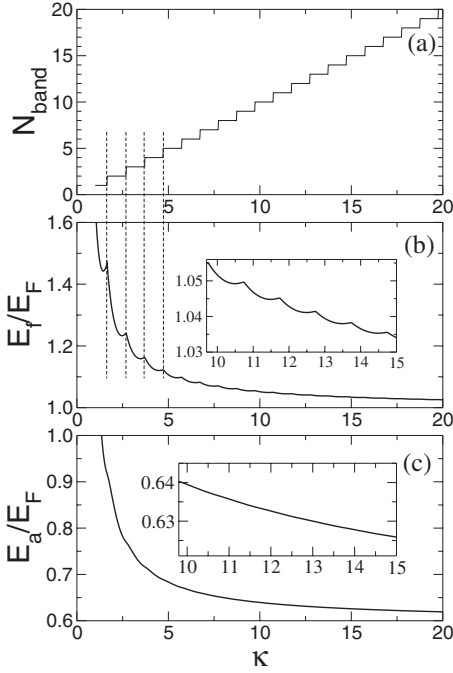


FIG. 5. (a) Number of subbands below the Fermi surface, (b) Fermi energy E_f , and (c) energy per electron E_a as a function of κ for a metallic thin film. Interfaces are modeled as infinite energy barriers. Insets show the enlarged portions of E_f and E_a for $\kappa \gg 1$. The dashed lines indicate the correspondence between the emergence of a new subband and a cusp.

$$S = \frac{4\kappa}{9N} + \frac{2(N+1)(2N+1)}{9\kappa^2} - \frac{N(N+1)(2N+1)(8N^2+3N-11)}{180\kappa^5}. \quad (22)$$

Although a film can change its thickness only monolayer by monolayer, we will first examine the properties of these energies assuming the film thickness could change continuously.

The film Fermi energy E_f is plotted in Fig. 5(b), where oscillations are clearly seen on top of a fast decreasing curve. The oscillations are marked by a series of cusps, which are the results of the emergence of new energy subbands below the Fermi level as the film thickness increases [see Fig. 5(b)]. As indicated by dashed lines in Fig. 5(b), two neighboring cusps are separated in the scaled thickness κ by about 1, $\Delta\kappa \approx 1$, which corresponds to $\Delta d \approx \lambda_F/2$ in real film thickness. This oscillation period can be understood as follows. Suppose that at thickness $d_1 \gg 1$, E_n just becomes the highest occupied subband. Then, at thickness $d_2 > d_1$, E_{n+1} emerges as the new highest occupied subband. Since the wave function for E_{n+1} has one more node than the wave function for E_n , we should have approximately for not-so-thin film ($\kappa \gg 1$)

$$\Delta d = d_2 - d_1 \approx \lambda_f/2 \approx \lambda_F/2, \quad (23)$$

where λ_f is the wavelength associated with the film Fermi energy E_f . This analysis clearly shows that the oscillations

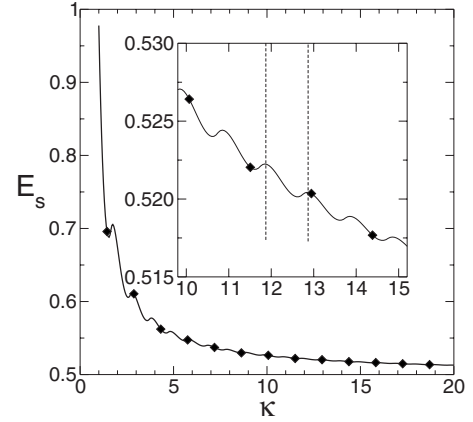


FIG. 6. Film interface energy E_s as a function of κ . Interfaces are modeled as infinite energy barriers. The inset shows the enlarged portion of E_s for large κ . The diamonds are the results for Pb(111) film. E_s is in units of $E_F k_F^2 / 4\pi$.

seen in the film Fermi energy E_f are caused by the discretization of energy bands due to the interface confinement.

In contrast, there are no oscillations in the energy per electron E_a , as shown in Fig. 5(c). The energy E_a is a very smooth decreasing function of κ (the scaled film thickness). According to criterion Eq. (17), this means that the islands in a film would always like to grow higher to lower its energy until the lateral dimensions of the islands become too small for them to be treated as two-dimensional islands. In other words, there would be no preferred island heights, contradicting the reports in Refs. 3, 4, and 7. Therefore, one concludes that the energy related to the contact area change and the side energy have to be accounted for and our theory of the free electron model does not apply to the situation depicted in Fig. 4. This conclusion is for all metals. In later discussions where interfaces are treated as finite energy barriers, it remains the same that there are no oscillations in E_a , affirming that our free electron model does not apply for films of islands.

It is a different story for continuous thin films, whose stability is determined by the film interface energy E_s . As seen in Fig. 6, there are oscillations in the film interface energy E_s as the result of discretization of energy band. This oscillatory behavior of E_s implies that the film can be stable for certain layers and unstable for other layers. The oscillatory difference between E_s and E_a is rooted mathematically in the relation

$$E_s \propto \kappa(E_a - 3E_F/5). \quad (24)$$

This relation shows that E_a has a steeper decreasing dependence on κ than E_s , which can iron out oscillations.

The E_s curve shown in Fig. 6 is universal for all metallic films up to some scaling constants. However, it does not mean that every metallic thin film has the same properties. In reality, a film can change its thickness only monolayer by monolayer. With a distinct layer spacing d_0 , each metallic film samples a different set of discrete points on the universal curve, which leads to different properties for each film. In Fig. 6, an example of such a sampling is given for Pb(111)

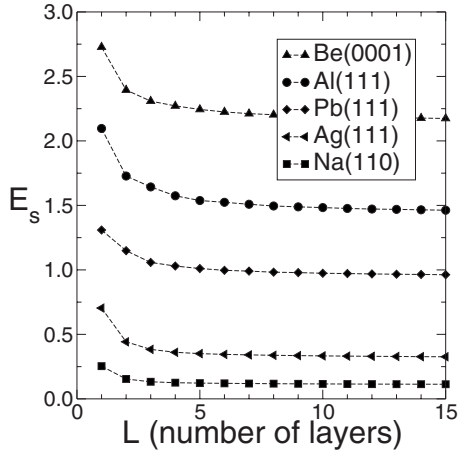


FIG. 7. Film interface energy E_s as a function of layer number L for metallic films: Be(0001), Al(111), Pb(111), Ag(111), and Na(110). E_s is in units of $\text{eV}/\text{\AA}^2$.

film. The results for more metallic films are plotted in Fig. 7 as a function of layer number L . To direct observation, there seems not much difference among these films besides a constant shift. However, more careful analysis with the second difference d^2E reveals sharp distinctions among films. For the five different metallic films shown in Fig. 7, their second differences are plotted in Fig. 8, revealing that the films are very different from each other.

For Ag(111) and Na(110), they become bulklike very quickly: beyond 5 monolayers ($L > 5$), their d^2E is already very small. This means that our calculations here fail to capture the experimental result in Ref. 1, where Ag(111) film of $L=7$ monolayers is very stable. Film Be(0001) is a little bit different: it decays into bulklike slower; despite the apparent oscillations, Be(0001) films of different monolayers are

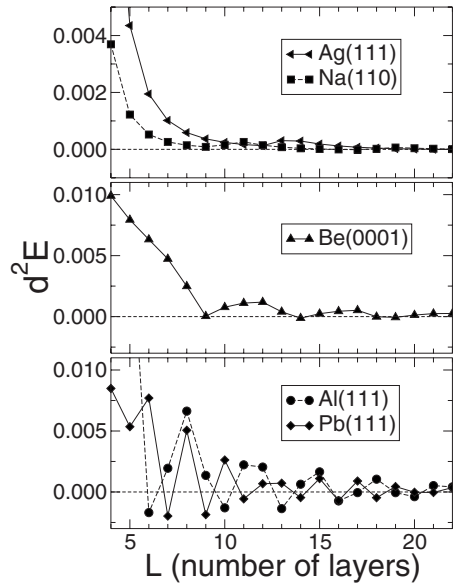


FIG. 8. The second difference d^2E as a function of layer number L for metallic films: Be(0001), Al(111), Pb(111), Ag(111), and Na(110). d^2E is in units of $\text{eV}/\text{\AA}^2$.

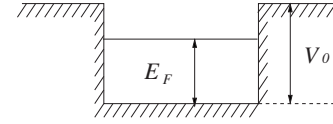


FIG. 9. Symmetric well of finite energy barriers.

stable since its second difference d^2E is almost always positive. Even its second difference d^2E becomes negative at a few thicknesses but its absolute value is very small and does not indicate strong instability. This implies that, according to this computation, it is very hard to grow atomically flat Be(0001) of any thickness in experiments.

Al(111) film and Pb(111) films are very different from the above three films. First, their second difference d^2E decays even slower. Second, their d^2E oscillate around zero with d^2E being possibly negative. For example, Al(111) film has negative d^2E at $L=5, 10, 13$, and 16 , which means that Al(111) film is unstable at these layers. In other words, unlike Be(0001), the oscillations here in d^2E imply oscillations in film stability for Al(111) film and Pb(111) film. Besides the apparent similarity, we observe that Al(111) film and Pb(111) film have different oscillation patterns in film stability. The stability of Pb(111) film oscillates in an even-odd fashion interrupted by crossovers. This is exactly the oscillation pattern observed in the stability of Pb(111) film in Ref. 15, although there is difference in which layers are stable. Considering how crude our model is, the agreement is quite amazing. Moreover, the amplitude of the oscillations in d^2E matches well with the *ab initio* calculations in Refs. 10, 15, 30, and 31. The oscillation pattern in film stability is determined by the ratio between the Fermi wavelength λ_F and the layer spacing d_0 as we discuss in the end. For Pb(111) film, we have $\lambda_F/2:d_0=1:1.44 \approx 2:3$; for Al(111) film, we have $\lambda_F/2:d_0=1:1.3 \approx 3:4$.

V. FINITE ENERGY BARRIER

In this section, we treat the interfaces as finite energy barriers. This is more realistic. First, a finite energy barrier allows charge spilling, reflecting the fact that there are always some electrons spilling over from metallic films into either semiconductor substrates or vacuum. Second, its height V_0 can be adjusted to reflect the nature of an interface. For an interface with vacuum, its height is $V_0=W_m+E_F$.

A. Symmetric wells

We shall first present a general study of symmetric wells and see how Fermi energy E_f , film interface energy E_s , and energy per electron E_a are influenced by the height V_0 of energy barrier. The results are applied later to metallic films.

For the symmetric well shown in Fig. 9, the discrete eigenenergies are

$$E_n = \frac{\eta_n^2}{\kappa^2} E_F, \quad (25)$$

where η_n is given by

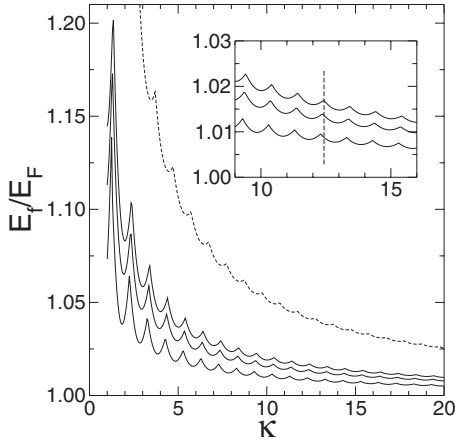


FIG. 10. Fermi energy E_f of thin films. The solid lines are for $V_0=2.2E_F$, $V_0=1.8E_F$, and $V_0=1.4E_F$ from top to bottom, respectively. The dashed curve is for the case of infinite barriers. The inset shows an enlarged portion of E_f curves.

$$\eta_n = n - \frac{2}{\pi} \sin^{-1} \left(\frac{\eta_n}{\kappa \sqrt{V_0/E_F}} \right). \quad (26)$$

With these subband energies, we can similarly compute the film Fermi energy E_f and the interface energy E_s .

The results are plotted in Figs. 10 and 11 for three barrier heights. We observe some general trends. As the energy barrier decreases, the energies (E_f and E_s) of the system decrease accordingly. At the same time, the slopes of the energies decreasing with thickness become less steep as V_0 decreases. This makes the oscillations in E_f and E_s appear more pronounced. These trends are the result of less confinement felt by free electrons as the barrier gets lower. In addition, as indicated by the dashed line in Fig. 10, the barrier height shifts the cusp positions, which is known as phase shift.²⁶

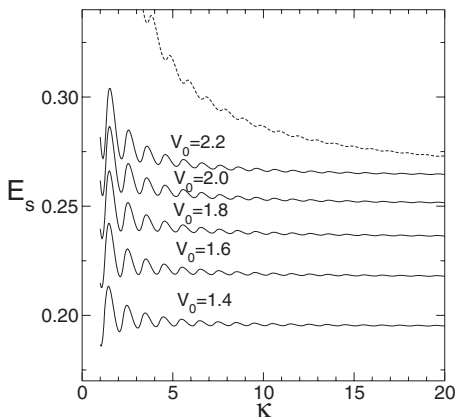


FIG. 11. Interface energy E_s of thin films. The solid lines are for $V_0=2.2E_F$, $V_0=2.0E_F$, $V_0=1.8E_F$, $V_0=1.6E_F$, and $V_0=1.4E_F$. The dashed curve is for the case of infinite barriers and is shifted downward by a trivial constant for easy comparison. The unit of E_s is $E_F^2 k_F^2 / 4\pi$.

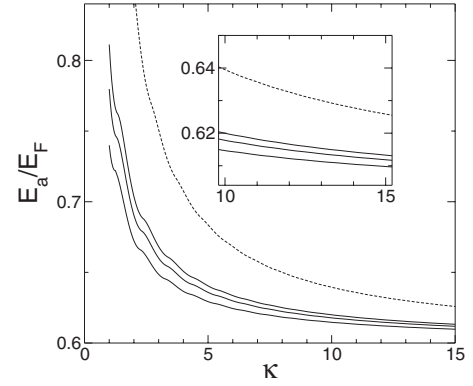


FIG. 12. Energy per electron E_a of thin films. The solid lines are for $V_0=2.2E_F$, $V_0=1.8E_F$, and $V_0=1.4E_F$ from top to bottom, respectively. The dashed curve is for the case of infinite barriers.

The energy per electron E_a is also computed and the results are plotted in Fig. 12. There are still no oscillations in E_a , further confirming that our free electron model with one-dimensional confinement does not apply to a film of islands shown in Fig. 4.

B. Freestanding films

With the symmetric square well of barrier height $V_0 = W_m + E_F$, the free electron model can be used to model a freestanding metallic film without any adjustable parameter. Although in experiments films are always grown on substrates, freestanding films are of great theoretical interests: they can serve as reference points to see how substrates affect film properties; furthermore, as indicated in the *ab initio* calculations in Refs. 10, 15, 30, and 31, the effect of substrates may only “phase shift” film properties.

We focus on the film interface energy E_s and its second difference. The results for five different metals (Be, Na, Pb, Ag, and Al) are plotted from Fig. 13 to Fig. 14–17, where the

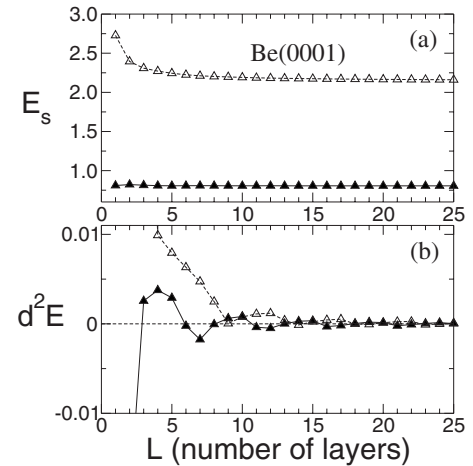


FIG. 13. Interface energy E_s and its second difference for a freestanding Be(0001) thin film. For Be, $W_m=4.98$ eV and $V_0=1.35E_F$. The open triangles with dashed lines are for infinite barriers. The unit of E_s is $\text{eV}/\text{\AA}^2$.

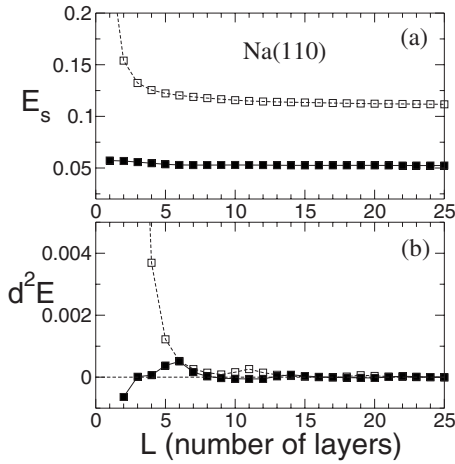


FIG. 14. Interface energy E_s and its second difference for a freestanding Na(110) thin film. For Na, $W_m=2.75$ eV and $V_0=1.85E_F$. The open squares with dashed lines are for infinite barriers. The unit of E_s is $\text{eV}/\text{\AA}^2$.

results with infinite barriers are also plotted for comparison.

The difference from infinite barriers is apparent. The interface energies E_s for these freestanding films become much smaller. In addition, for infinite barriers, there is a sharp increase in interface energies E_s as the thickness of metallic thin film goes below 5 monolayers. This sharp increase is leveled for finite energy barriers; as a result, all the five metallic films become unstable for certain layer numbers smaller than 5. These differences agree with the general trends discussed in the last subsection; they are the result of the less confinement of finite energy barriers, which allow the electron to spill over into the vacuum to reduce their kinetic energy.

For relatively thicker films, where the confinement is reduced by larger thickness, the difference between the infinite barrier and finite barrier becomes less severe. This is clear in the second difference d^2E from Fig. 13 to Fig. 17 for films

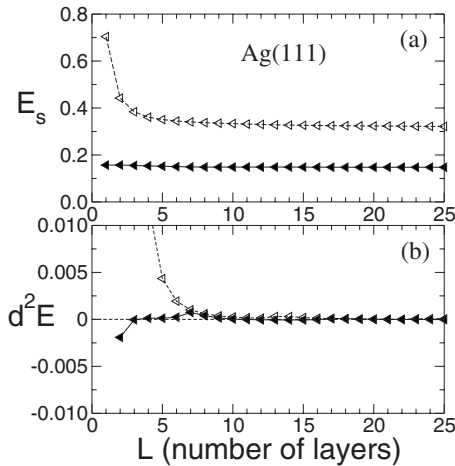


FIG. 15. Interface energy E_s and its second difference for a freestanding Ag(111) thin film. For Ag, $W_m=4.3$ eV and $V_0=1.78E_F$. The open triangles with dashed lines are for infinite barriers. The unit of E_s is $\text{eV}/\text{\AA}^2$.

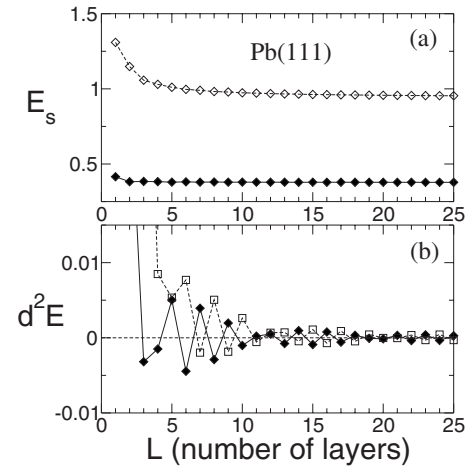


FIG. 16. Interface energy E_s and its second difference for a freestanding Pb(111) thin film. For Pb, $W_m=4.25$ eV and $V_0=1.45E_F$. The open diamonds with dashed lines are for infinite barriers. The unit of E_s is $\text{eV}/\text{\AA}^2$.

with layer numbers larger than 5. For Be(0001), Na(110), and Ag(111), the second difference d^2E is again very small for $L>5$, implying that these films become bulklike very quickly as they grow thicker. We note that freestanding film Be(0001) is quite unstable at $L=7$. For Pb(111) film, the odd-even oscillations persist in d^2E with a similar amplitude. The effect of finite energy barrier is only to phase shift the oscillations by 1 monolayer, as seen in Fig. 16. In Fig. 17, the Al(111) film also has oscillations with a similar pattern in d^2E .

Overall, very thin films ($L<5$) are greatly influenced by the finiteness of the energy barriers. However, as we mentioned earlier, free electron models are unlikely to capture accurately the properties of a very thin film. Therefore, it is reasonable to conclude that the effect of energy barrier height is small; there is no essential difference between the

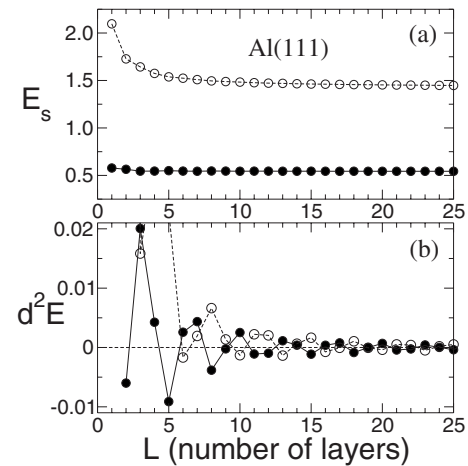


FIG. 17. Interface energy and its second difference of a freestanding Al(111) thin film. For Al, $W_m=4.28$ eV and $V_0=1.37E_F$. The open circles with dashed lines are for infinite barriers. The unit of E_s is $\text{eV}/\text{\AA}^2$.

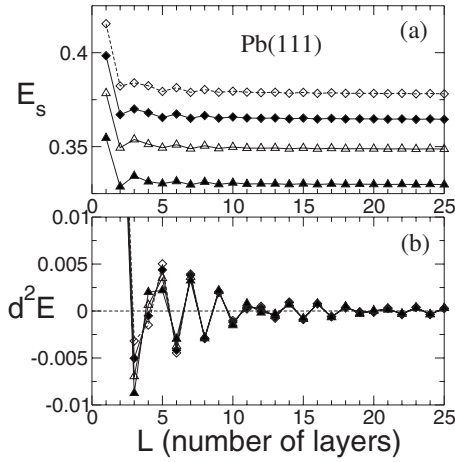


FIG. 18. Interface energy E_s and its second difference of Pb(111) thin films on semiconductor substrates. From top to bottom in (a), the results are for $V_2 = 1.45E_F = V_1$ (open diamonds), $V_2 = 1.34E_F$ (solid diamonds), $V_2 = 1.22E_F$ (open triangles), and $V_2 = 1.11E_F$ (solid triangles). The unit of E_s is $\text{eV}/\text{\AA}^2$.

infinite energy barrier and finite energy barrier.

C. Semiconductor substrate

In experiments, films are grown on substrates, which influence the film growth in many different aspects, for example, film orientation. We are here interested in how substrates affect the stability of metallic thin films.

For a metallic thin film on a semiconductor substrate, the electrons inside the film experience two energy barriers: one at the vacuum interface with a height of $V_1 = W_m + E_F$ and the other at the semiconductor side of a height V_2 ($E_F < V_2 < V_1$) that depends on the substrate. In the free electron model, the film is modeled as electrons residing in an asymmetric well, as shown in Fig. 2. In an asymmetric well, the energy levels are given by

$$E_n = \frac{\eta_n^2}{\kappa^2} E_F, \quad (27)$$

where η_n satisfies

$$\frac{\eta_n(\sqrt{\kappa^2 V_1/E_F - \eta_n^2} + \sqrt{\kappa^2 V_2/E_F - \eta_n^2})}{\eta_n^2 - \sqrt{(x^2 V_1/E_F - \eta_n^2)(x^2 V_2/E_F - \eta_n^2)}} = \tan(\eta_n \pi). \quad (28)$$

Similarly, with these energy levels, we have performed computation for the five metallic thin films, Na, Pb, Al, Ag, and Be. The effect of a substrate is marginal compared to the freestanding films. As an example, the results for Pb(111) film are shown in Fig. 18. As V_2 changes, reflecting a possible change of substrates, the interface energy E_s does not change much except a trivial constant shift. This is more evident in the second difference d^2E , which only sees a slight change in its magnitude.

VI. ELECTRONS IN A CORRUGATED BOX

We have so far completely ignored the lattice potential. However, studies in quantum well states^{26,27} show that, to

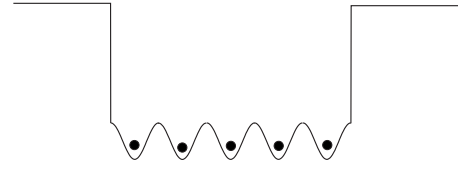


FIG. 19. Corrugated potential well.

understand some basic experimental observations, one needs a model of particle in a corrugated box, where the lattice potential perpendicular to the film is added, as shown in Fig. 19. It motivates us to examine this model and see how the lattice potential affects the stability of metallic thin films.

Without loss of essential physics, we choose the corrugated periodic potential to be a simple cosine function, that is,

$$V_c(z) = v \cos \frac{2\pi z}{d_0}, \quad (29)$$

where v is the lattice potential strength and will be treated as a free parameter. Without any confinement, a system with potential $V_c(z)$ possesses Bloch states and continuous Bloch energy bands. For a metallic thin film, there is confinement by the two interfaces at $z=0$ and $z=d=Ld_0$. As a result, the Bloch bands are discretized. In general, the eigenstates of this system has the following form:

$$\Phi_k(z) = A e^{ikz} \phi_k(z) + B e^{-ikz} \phi_k(-z), \quad (30)$$

where $\phi_k(z)$ is a periodic function of period d_0 . The discretized value of k and the two parameters, A and B , are to be determined by the boundary conditions at the interfaces $z=0$ and $z=d$ (for details see the Appendix).

Here, we consider only the symmetric case, where the two energy barriers at the interfaces are of the same height V_0 . As we have noted in the previous sections, the barrier height has very limited effect on the film stability for $L > 5$. Therefore, we will concentrate on the case of infinite energy barrier and only briefly examine the case of finite energy barrier.

We present the results for Pb(111) film as an example. The subband energies of Pb(111) film are plotted in Fig. 20, while its interface energies E_s are shown in Fig. 21. The most interesting feature is that if the film thickness is allowed to change continuously, the energy E_s oscillates with period of d_0 , the layer spacing. However, these oscillations do not show up in E_s since the real Pb(111) film changes its thickness only monolayer by monolayer, as seen in Fig. 18.

The interface energies E_s and its second difference for three metallic films, Pb(111), Al(111), and Be(0001), are plotted in Figs. 22–24. There is no substantial change in the stability of these films. Their second difference d^2E holds the same oscillation patterns. There is only change in exactly which layer is stable or unstable, which is hard to be captured by a model as crude as the free electron model. The same conclusion holds for other metallic films.

The effect of finite energy barrier is similar to the model of particle in a box. The film of less than 5 monolayers is affected greatly, while thicker films experience little change.

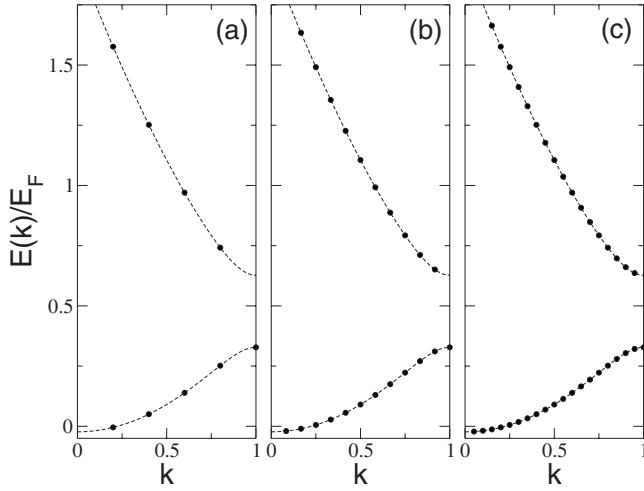


FIG. 20. Subband energy in Pb(111) film with a corrugated potential. (a) 5 monolayers, (b) 12 monolayers, and (c) 20 monolayers. The dashed line represents the Bloch bands without any confinement. $v=0.3E_F$ in Eq. (29). The Bloch wave vector k is in units of π/κ_0 with $\kappa_0=k_F d_0/\pi$.

As an example, the results for Pb(111) film are shown in Fig. 25.

VII. DISCUSSION AND SUMMARY

We have presented a systematic and detailed study of the stability of metallic thin films with free electron models. Our study has shown two consistent findings. On one hand, if there are oscillations in the film stability (in terms of interface energy E_s and in particular the second difference d^2E) the oscillation pattern is very robust against the modification of energy barriers and the addition of a lattice potential. On the other hand, the stability of a film of a given thickness is quite sensitive to barrier heights and lattice potential. This kind of sensitivity indicates that the free electron model lacks the power to predict at exactly what thickness the film is stable. These two findings can be understood as follows.

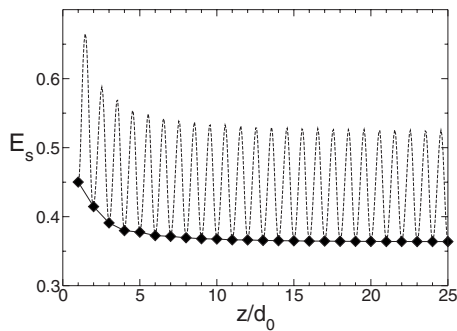


FIG. 21. Interface energy of Pb(111) film. The discrete set of diamonds are for real Pb(111) film, whose thickness changes only monolayer by monolayer. The dashed line is for the case where the film thickness is allowed to change continuously. $v=0.3E_F$. The unit of E_s is $E_F k_F^2/4\pi$.

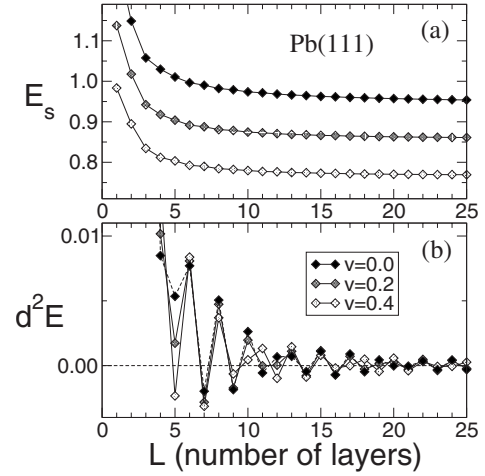


FIG. 22. Interface energy and its second difference of Pb(111) film. (a) Surface energy E_s for $v=0.0$, $v=0.2E_F$, and $v=0.4E_F$ from top to bottom. (b) The second difference d^2E . The unit is $\text{eV}/\text{\AA}^2$.

The robustness of the oscillation pattern in the film stability is rooted in the discretization of energy bands in metallic thin films. For a metallic thin film, the energy bands become discretized due to the confinement at the two interfaces. As the film thickness grows, new subbands emerge under the Fermi level periodically, producing oscillations in the interface energy E_s with period around half the Fermi wavelength, $\lambda_F/2$ [see the argument leading to Eq. (23)]. This periodic oscillation is robust against the choices of energy barriers and existence of lattice potential since the discretization always exists as long as the electrons are confined by the two interfaces. Moreover, as we carefully examine the arguments leading to Eq. (23), we find that the arguments are general for not-very-thin films and do not depend on the details of the free electron model. This means that the oscillation period is also robust, being around $\lambda_F/2$. This periodic oscillation in E_s interplays with another periodic change, the monolayer by monolayer growth of film thickness, leading to

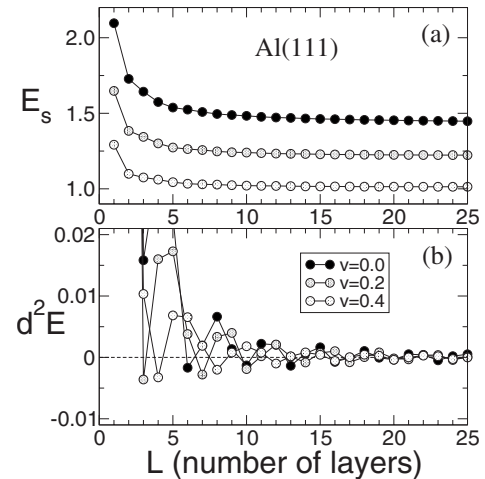


FIG. 23. Interface energy and its second difference of Al(111) film. (a) Surface energy E_s for $v=0.0$, $v=0.2E_F$, and $v=0.4E_F$ from top to bottom. (b) The second difference d^2E . The unit of E_s is $\text{eV}/\text{\AA}^2$.

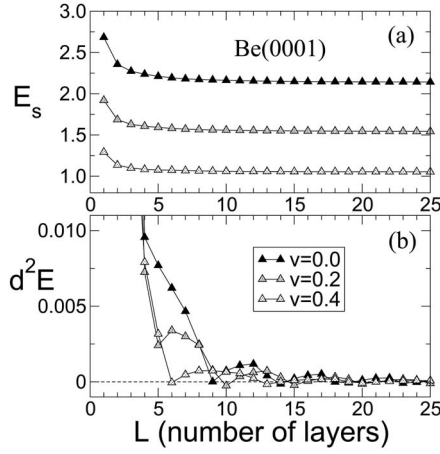


FIG. 24. Interface energy and its second difference of Be(0001) film. (a) Surface energy E_s for $v=0.0$, $v=0.2E_F$, and $v=0.4E_F$ from top to bottom. (b) The second difference d^2E . The unit of E_s is $\text{eV}/\text{\AA}^2$.

a possible oscillation pattern in the film stability. The oscillation pattern is determined by the ratio between the Fermi wavelength λ_F and the layer spacing d_0 . For Pb(111) film, we have $\lambda_F/2:d_0=1:1.44 \approx 2:3$, which gives us the even-odd oscillations; for Al(111) film, we have $\lambda_F/2:d_0=1:1.3 \approx 3:4$, which leads to another oscillation pattern.

However, the ratio $\lambda_F/2:d_0$ only determines the oscillation pattern in film stability. It does not tell at what thickness a film is stable, which is decided by the phase of the oscillations. As we have shown, the phase is quite sensitive to the heights of energy barriers and lattice potential. This is why the stability of a film of certain thickness is quite sensitive to details of the free electron model. As the free electron model is very crude and many details of a given metal are ignored, it is unlikely that this simple model can produce accurately the phase of the oscillations, predicting at what thickness a film is stable.

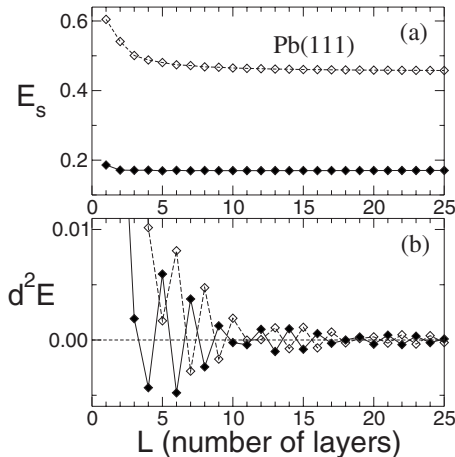


FIG. 25. Interface energy and its second difference of Pb(111) film. (a) Surface energy and (b) its second difference d^2E . Open squares are for infinite barriers; solid circles are for the free standing case with $V_0=1.45E_F$. $v=0.1E_F$. The unit is $\text{eV}/\text{\AA}^2$.

Overall, we conclude that the free electron model captures very well the physics relating to the discretization of energy bands. As a result, it can predict quite accurately the oscillation pattern in the film stability. However, it is not good at predicting exactly at what thickness a film is stable.

At the end, we want to mention that another kind of oscillations may arise in determining film stability. They are the Friedel oscillations in the electron density, which leads to an oscillatory mean-field potential for electrons via Coulomb interaction. This mean-field potential, which is completely neglected in the free electron model, can be important and also create an oscillation in the interface energy E_s . Similarly, this oscillation can interplay with the period of layer spacing, producing an oscillation pattern in the film stability. What is interesting is that the Friedel oscillations are also of period of half Fermi wavelength $\lambda_F/2$. It makes it hard to separate between the physics relating to Friedel oscillations and energy discretization. More detailed theoretical study and experiments are needed.

ACKNOWLEDGMENTS

We thank Yu Jia and Hanno Weitering for helpful discussions. This work is supported in part by NSF Grants Nos. DMR-0325218 and DMR-0606485, by DOE Grant No. DE-FG02-05ER46209, and in part by the Division of Materials Sciences and Engineering, Office of Basic Energy Sciences, DOE. This work is also supported by the ‘‘BaiRen’’ program of Chinese Academy of Sciences, the NSF of China (10504040), and the 973 project of China (2005CB724500 and 2006CB921400).

APPENDIX: FREE ELECTRON IN A PERIODIC BOX

In this appendix, we describe in detail how the wave function in Eq. (30) for a free electron in a periodic box is computed. The Schrödinger equation is

$$-\frac{\hbar^2}{2m} \frac{d^2}{dz^2} \psi + V(z)\psi = E\psi, \quad (\text{A1})$$

where the potential V is

$$V(z) = \begin{cases} V_0, & z < 0 \text{ or } z > a \\ V_c(z) & \text{otherwise.} \end{cases} \quad (\text{A2})$$

Since $V_c(z)$ is symmetric, that is, $V_c(z)=V_c(-z)$. This implies that if $\Psi(z)$ is a solution for eigenenergy E , so is $\Psi(-z)$. In general, these two solutions are independent of each other; therefore, a general solution can be written in the form

$$\Phi_k(z) = Ae^{ikz}\phi_k(z) + Be^{-ikz}\phi_k(-z), \quad (\text{A3})$$

where $\phi_k(z)$ is a periodic function of d_0 . The coefficients A and B are to be determined by the boundary conditions. Since we are only interested in the bands below the energy barriers at the interfaces, the boundary conditions are

$$\left. \frac{\Phi'(z)}{\Phi(z)} \right|_{z=0 \text{ or } a} = -\tilde{k}, \quad (\text{A4})$$

where $\tilde{k} = \sqrt{2m(V_0 - E)}/\hbar$. In the case $V_0 = \infty$, it reduces to $\Phi(z)|_{z=0 \text{ or } a} = 0$. In our method, we initially guess a k and

compute numerically to find the corresponding eigenenergy E and eigenstate $\phi_k(z)$. With the results, we check if the above boundary conditions can be satisfied. If not, we modify k and repeat until the boundary conditions are met.

Two cautions have to be taken. First, since the periodic potential has a finite range, the wave number k can be complex.³⁸ Second, at the Brillouin zone center and edge, one has $\Psi(-z) = \pm \Psi(z)$, indicating that $\Psi(z)$ and $\Psi(-z)$ are no longer independent of each other. For this case, the general solution takes the following form:

$$\Phi(z) = cz\phi_0(z) + \psi(z), \quad (\text{A5})$$

where $\phi_0(z)$ is the Bloch wave solution at either the zone center or edge and $\psi(z)$ is a periodic function satisfying

$$-\frac{\hbar^2 d^2 \psi}{2mdz^2} + V(z)\psi - \mathcal{E}\psi = \frac{c\hbar^2 d\phi_0}{m dz}. \quad (\text{A6})$$

Further mathematical details can be found in Ref. 38 and another book by Whittaker and Watson.³⁹

¹A. R. Smith, K.-J. Chao, Q. Niu, and C.-K. Shih, *Science* **273**, 226 (1996).
²L. Gavioli, K. R. Kimberlin, M. C. Tringides, J. F. Wendelken, and Z. Y. Zhang, *Phys. Rev. Lett.* **82**, 129 (1999).
³K. Budde, E. Abram, V. Yeh, and M. C. Tringides, *Phys. Rev. B* **61**, R10602 (2000).
⁴V. Yeh, L. Berbil-Bautista, C. Z. Wang, K. M. Ho, and M. C. Tringides, *Phys. Rev. Lett.* **85**, 5158 (2000).
⁵M. Hupalo, V. Yeh, L. Berbil-Bautista, S. Kremmer, E. Abram, and M. C. Tringides, *Phys. Rev. B* **64**, 155307 (2001).
⁶M. Hupalo, S. Kremmer, V. Yeh, L. Berbil-Bautista, E. Abram, and M. C. Tringides, *Surf. Sci.* **493**, 526 (2001).
⁷W. B. Su, S. H. Chang, W. B. Jian, C. S. Chang, L. J. Chen, and T. T. Tsong, *Phys. Rev. Lett.* **86**, 5116 (2001).
⁸S. H. Chang, W. B. Su, W. B. Jian, C. S. Chang, L. J. Chen, and T. T. Tsong, *Phys. Rev. B* **65**, 245401 (2002).
⁹H. Okamoto, D. Chen, and T. Yamada, *Phys. Rev. Lett.* **89**, 256101 (2002).
¹⁰H. Hong, C.-M. Wei, M. Y. Chou, Z. Wu, L. Basile, H. Chen, M. Holt, and T.-C. Chiang, *Phys. Rev. Lett.* **90**, 076104 (2003).
¹¹W. B. Su, S. H. Chang, H. Y. Lin, Y. P. Chiu, T. Y. Fu, C. S. Chang, and T. T. Tsong, *Phys. Rev. B* **68**, 033405 (2003).
¹²J. H. Dil, J. W. Kim, S. Gokhale, M. Tallarida, and K. Horn, *Phys. Rev. B* **70**, 045405 (2004).
¹³C.-S. Jiang, S.-C. Li, H.-B. Yu, D. Eom, X.-D. Wang, P. Ebert, J.-F. Jia, Q.-K. Xue, and C.-K. Shih, *Phys. Rev. Lett.* **92**, 106104 (2004).
¹⁴A. Crottini, D. Cvetko, L. Floreano, R. Gotter, A. Morgante, and F. Tommasini, *Phys. Rev. Lett.* **79**, 1527 (1997).
¹⁵M. M. Özer, Y. Jia, B. Wu, Z. Y. Zhang, and H. H. Weitering, *Phys. Rev. B* **72**, 113409 (2005).
¹⁶Y. Guo, Y.-F. Zhang, X.-Y. Bao, T.-Z. Han, Z. Tang, L.-X. Zhang, W.-G. Zhu, E. Wang, Q. Niu, Z. Qiu, J.-F. Jia, Z.-X. Zhao, and Q.-K. Xue, *Science* **306**, 1915 (2004).
¹⁷M. M. Özer, J. R. Thompson, and H. H. Weitering, *Nat. Phys.* **2**, 173 (2006).
¹⁸Y.-F. Zhang, J.-F. Jia, T.-Z. Han, Z. Tang, Q.-T. Shen, Y. Guo, Z. Q. Qiu, and Q.-K. Xue, *Phys. Rev. Lett.* **95**, 096802 (2005).
¹⁹X.-Y. Bao, Y.-F. Zhang, Y. Wang, J.-F. Jia, Q.-K. Xue, X. C. Xie, and Z.-X. Zhao, *Phys. Rev. Lett.* **95**, 247005 (2005).
²⁰T. Z. Han, G. C. Dong, Q. T. Shen, Y. F. Zhang, J. F. Jia, and Q. K. Xue, *Appl. Phys. Lett.* **89**, 183109 (2006).
²¹L. Y. Ma, L. Tang, Z. L. Guan, K. He, K. An, X. C. Ma, J. F. Jia, Q. K. Xue, Y. Han, S. Huang, and F. Liu, *Phys. Rev. Lett.* **97**, 266102 (2006).
²²Y. Qi, X. C. Ma, P. Jiang, S. H. Ji, Y. S. Fu, J. F. Jia, Q. K. Xue, and S. B. Zhang, *Appl. Phys. Lett.* **90**, 013109 (2007).
²³A. Mans, J. H. Dil, A. R. H. F. Ettema, and H. H. Weitering, *Phys. Rev. B* **72**, 155442 (2005).
²⁴Zhenyu Zhang, Qian Niu, and C.-K. Shih, *Phys. Rev. Lett.* **80**, 5381 (1998).
²⁵Z. Y. Zhang, *Surf. Sci.* **571**, 1 (2004).
²⁶T. C. Chiang, *Surf. Sci. Rep.* **39**, 181 (2000).
²⁷Z. Q. Qiu and N. V. Smith, *J. Phys.: Condens. Matter* **14**, R169 (2002).
²⁸M. Milun, P. Pervan, and D. P. Woodruff, *Rep. Prog. Phys.* **65**, 99 (2002).
²⁹N. Trivedi and N. W. Ashcroft, *Phys. Rev. B* **38**, 12298 (1988).
³⁰C. M. Wei and M. Y. Chou, *Phys. Rev. B* **66**, 233408 (2002).
³¹Y. Jia, B. Wu, H. H. Weitering, and Zhenyu Zhang, *Phys. Rev. B* **74**, 035433 (2006).
³²N. W. Ashcroft and N. D. Mermin, *Solid State Physics* (Sanders, Philadelphia, 1976).
³³F. Seitz, *The Modern Theory of Solids* (McGraw-Hill, New York, 1940).
³⁴It is called surface energy in some literature, for example, Refs. 30.
³⁵S. G. Louie and M. L. Cohen, *Phys. Rev. B* **13**, 2461 (1976).
³⁶J. Tersoff, *Phys. Rev. Lett.* **52**, 465 (1984).
³⁷D.-A. Luh, T. Miller, J. J. Paggel, M. Y. Chou, and T.-C. Chiang, *Science* **292**, 1131 (2001).
³⁸N. W. McLachlan, *Theory and Application of Mathieu Functions* (Oxford, New York, 1947).
³⁹E. T. Whittaker and G. N. Watson, *A Course of Modern Analysis* (Cambridge University, Cambridge, 1927).